Recognition of Sequence-Directed DNA Structure by the Klenow Fragment of DNA Polymerase I†

Theodore E. Carver, Jr.,‡ and David P. Millar*

Department of Molecular Biology, MB-19, The Scripps Research Institute, 10550 North Torrey Pines Road, La Jolla, California 92037

Received August 22, 1997; Revised Manuscript Received December 5, 1997

ABSTRACT: Time-resolved fluorescence spectroscopy was used to investigate the influence of sequence-directed DNA structure upon the interaction between the Klenow fragment of DNA polymerase I and a series of defined oligonucleotide primer/templates. 17/27-mer (primer/template) oligonucleotides containing a dansyl fluorophore conjugated to a modified deoxyuridine residue within the primer strand were used as substrates for binding to Klenow fragment. The time-resolved fluorescence anisotropy decay of the dansyl probe was analyzed in terms of two local environments, either solvent-exposed or buried, corresponding to primer/templates positioned with the primer 3′ terminus in the polymerase site or the 3′-5′ exonuclease site of the enzyme, respectively. Equilibrium constants for partitioning of DNA between the two sites were evaluated from the anisotropy decay data for primer/templates having different (A+T)-rich sequences flanking the primer 3′ terminus. Primer/templates with AAAATG/TTTTAC and CGATAT/GCTATA terminal sequences (the nucleotides on the left refer to the last six bases at the 3′ end of the primer, and the nucleotides on the right are the corresponding bases in the template) were bound mostly at the polymerase site. The introduction of single mismatches opposite the primer 3′ terminus of these DNA substrates increased their partitioning into the 3′-5′ exonuclease site, in accord with the results of an earlier study [Carver, T. E., Hochstrasser, R. A., and Millar, D. P. (1994) *Proc. Natl. Acad. Sci. U.S.A. 91*, 10670−10674]. In contrast, a primer/template with the terminal sequence CAATTT/GTTAAA, containing an A-tract element AATTT, exhibited a surprising preference for binding at the 3′-5′ exonuclease site, despite the absence of mismatched bases in the DNA substrate. Interruption of the A-tract with a single AG step, to give the terminal sequence CAGTTT/GTCAAA, reversed the effect of the A-tract, causing the DNA to partition in favor of the polymerase site. Moreover, the presence of a single mismatch opposite the primer 3′ terminus was also sufficient to reverse the effect of the A-tract, resulting in a distribution of DNA between polymerase and 3′-5′ exonuclease sites that was similar to that observed for the other mismatched DNA substrates. Taken together, these results suggest that the A-tract adopts an unusual conformation that is disruptive to binding at the polymerase site. The effect of the A-tract on binding of DNA to the polymerase site is discussed in terms of the unusual helix structural parameters associated with these sequence elements and the difference between the local geometry of the A-tract and the conformation adopted by duplex DNA within the polymerase cleft. The results of this study show that in addition to base mismatches, Klenow fragment can also recognize irregularities in the helix geometry of perfectly base-paired DNA.

DNA polymerases are the primary enzymes responsible for the accurate replication of DNA in vivo. Faithful replication of DNA is a result of (1) selection of the correct deoxynucleotide during polymerization, (2) inefficient extension from a mispaired primer 3′ terminus, and (3) preferential excision of mismatched bases from the primer terminus by a proofreading 3′-5′ exonuclease activity (reviewed in *1*−*3*). Although the fidelity of DNA polymerases is quite high during the replication of almost all DNA, there are significant variations in misinsertion rates and proofreading efficiencies, depending upon the sequence of the DNA surrounding the primer 3′ terminus (*4*−*8*). These effects have frequently been correlated with the thermodynamic properties of different nucleotide sequences in double-stranded DNA. For example, sequence-dependent variations in nucleotide insertion kinetics have been attributed to differences in base stacking energies between an incoming deoxynucleoside triphosphate molecule and the 3′ terminal base of the DNA primer/template (*7*). In addition, Petruska and Goodman (*4*) have proposed that the efficiency of exonucleolytic proofreading of a 3′ terminal base is governed by the relative proportions of A·T and G·C base pairs in the adjacent duplex region. This model is based on the observation that the preferred substrate for 3′-5′ exonuclease activity is single-stranded DNA, implying that melting of the duplex terminus is required for exonucleolytic degradation of a double-stranded DNA substrate (*9*). The requirement for duplex

† Supported by a grant from the National Institutes of Health (GM44060 to D.P.M.) and a postdoctoral fellowship from the National Institutes of Health (GM15729 to T.E.C.).

* Corresponding author.

‡ Present address: Argonne National Laboratory, Argonne, IL 60439.

S0006-2960(97)02084-9 CCC: $15.00
Published on Web 01/27/1998

melting has been directly confirmed by crystallographic (*10*, *11*) and solution (*12*) studies.

In addition to variations in thermodynamic parameters, the base sequence can also exert a significant influence on the local geometry of the DNA double helix. Investigations of DNA structure during the past decade have shown that significant sequence-dependent deviations from the canonical B-form helical structure can occur. These differences, although small relative to differences between the "A", "B," and "Z" DNA structures, can have a pronounced effect upon sequence-independent enzymes that use duplex DNA as a substrate (*13*, *14*). Sequence-directed DNA curvature is correlated with a variety of protein−DNA interactions in vivo, and DNA bending may be important in sequence recognition by DNA-binding proteins (*15*). The effects of these sequence-dependent structural phenomena upon the interactions of DNA polymerases with DNA substrates have not been investigated.

The Klenow fragment of DNA polymerase I contains both 5′-3′ DNA polymerase and 3′-5′ exonuclease activities, spatially separated in distinct structural domains (reviewed in *16*). The Klenow fragment is an attractive model system for structure−function studies of a DNA replication enzyme, owing to the availability of high-resolution crystal structures of the enzyme (*17*) and its complexes with DNA substrates (*10*, *11*). In a previous study, we used a spectroscopic marker attached to DNA to investigate the interaction of mispaired DNA substrates with Klenow fragment (*18*). Time-resolved fluorescence anisotropy decays of duplex DNA labeled with a dansyl probe were used to monitor the modes of binding of different mispaired DNAs to the DNA polymerase, demonstrating that mispaired sequences tend to partition in favor of the proofreading 3′-5′ exonuclease site.

In the present work, we use the time-resolved fluorescence anisotropy technique to examine the effects of different matched (A+T)-rich sequences upon the partitioning of DNA substrates between the polymerase and 3′-5′ exonuclease sites of Klenow fragment. Our results demonstrate that the presence of an A-tract sequence element can significantly increase the partitioning of a DNA substrate into the 3′-5′ exonuclease site, despite the absence of mismatched bases within the DNA, suggesting that these sequences cause the base-paired duplex terminus to adopt a structure that is disruptive to binding at the polymerase site. Such effects may contribute to sequence-dependent variations in the enzymatic activity of DNA polymerases as they copy natural DNA templates.

MATERIALS AND METHODS

Materials. The D424A (Asp to Ala at position 424) exonuclease-deficient mutant of the Klenow fragment of DNA polymerase I was purified as described previously (*19*). This protein was found to have no detectable 3′-5′ exonuclease activity upon matched and mismatched DNA substrates over a 30 min time period, showing that the samples were stable over the time required for time-correlated single-photon counting measurements. Dansyl-labeled 17-mer oligonucleotides and unlabeled 27-mer oligonucleotides (Table 1) were synthesized using standard β-cyanoethyl phosphoramidite chemistry and purified using reverse-phase HPLC as described (*20*). DNA duplexes were annealed by heating a mixture of the dansyl-labeled 17-mer and a 1.2-fold molar excess of the 27-mer strands at 80 °C and allowing the solution to cool slowly to room temperature.

Table 1: Fluorescent DNA Substrates[a]

1	5′-TCGCAGCCG**X**CAAAATG 3′-AGCGTCGGCAGTTTTACATATAGCCGA
2	5′-TCGCAGCCG**X**CAAAATG 3′-AGCGTCGGCAGTTTTA$_G$ATATAGCCGA
3	5′-TCGCAGCCG**X**CCGATAT 3′-AGCGTCGGCAGGCTATAATATAGCCGA
4	5′-TCGCAGCCG**X**CCGATAT 3′-AGCGTCGGCAGGCTAT$_T$ATATAGCCGA
5	5′-TCGCAGCCG**X**CCAATTT 3′-AGCGTCGGCAGGTTAAAATATAGCCGA
6	5′-TCGCAGCCG**X**CCAATTT 3′-AGCGTCGGCAGGTTAA$_T$ATATAGCCGA
7	5′-TCGCAGCCG**X**CCAGTTT 3′-AGCGTCGGCAGGTCAAAATATAGCCGA

[a] X denotes a deoxyuridine residue, labeled at the C5 position with a dansyl fluorophore.

Time-Resolved Fluorescence Spectroscopy. Fluorescence decay measurements were performed using the time-correlated single photon counting setup described in detail elsewhere (*21*). Samples were measured in quartz cuvettes and excited at 318 nm using the vertically polarized output from a frequency-doubled synchronously mode-locked DCM dye laser (Coherent 702). The dansyl emission was monitored at 535 nm using a monochromator (JY H-10) and a microchannel plate photomultiplier (Hamamatsu R2809U-01). Time-resolved emission profiles were acquired using standard time-correlated single photon counting electronics (Ortec and Tennelec). Decays were recorded in 512 channels of a multichannel analyzer (Ortec Norland 5510) using a sampling time of 88 ps per channel. The instrument response function, measured by scattering the laser pulses from a suspension of nondairy coffee creamer, had a full width at half-maximum of 45 ps. For measurement of fluorescence anisotropy decay, a polarizer in the emission path was alternated between vertical and horizontal directions every 15 s, and the decays collected with each polarizer setting were accumulated in separate memory segments of the multichannel analyzer. Movement of the polarizer and data accumulation in the multichannel analyzer were under computer control. All measurements were performed at 20 °C. Time-resolved emission data were transferred to a Sparc LX workstation for analysis.

Data Analysis. The time-dependent fluorescence anisotropy, $r(t)$, was computed directly from polarized components of the time-resolved fluorescence:

$$r(t) = \frac{I_{||}(t) - I_{\perp}(t)}{I_{||}(t) + 2I_{\perp}(t)} \quad (1)$$

where $I_{||}(t)$ and $I_{\perp}(t)$ are the intensity decays measured with the emission polarizer oriented parallel or perpendicular to the excitation polarization, respectively. Equation 1 does not allow for convolution with the instrument response. However, convolution effects were negligible in the present measurements owing to the very narrow width of the instrument response function (45 ps) and the relatively slow

time scale of the motions involved (in the nanosecond range, see Results).

The anisotropy decay data were fitted to an expression incorporating the fluorescence lifetimes, rotation times, and associated amplitudes for two states of the dansyl probe. In previous work, we showed that a dansyl probe seven bases upstream from the primer 3′ terminus can experience two environments, either solvent-exposed or buried, depending upon the location of the primer 3′ terminus within the enzyme (*18*, *21*). Specifically, the exposed probes correspond to DNA primer/templates bound to Klenow fragment with the primer 3′ terminus in the polymerase active site, and the buried probes correspond to bound primer/templates with the 3′ terminus at the 3′-5′ exonuclease site. Accordingly, the observed time-dependent fluorescence anisotropy is the sum of contributions from the exposed state, $r_e(t)$, and the buried state, $r_b(t)$:

$$r(t) = f_e(t)r_e(t) + f_b(t)r_b(t) \quad (2)$$

where the fractional contribution of exposed probes to the fluorescence anisotropy at time t, $f_e(t)$, is given by

$$f_e(t) = \frac{x_e\sum_{i=1}^{N_e}\alpha_{ie}\exp(-t/\tau_{ie})}{x_e\sum_{i=1}^{N_e}\alpha_{ie}\exp(-t/\tau_{ie}) + x_b\sum_{i=1}^{N_b}\alpha_{ib}\exp(-t/\tau_{ib})} \quad (3)$$

where τ_{ie}, α_{ie}, N_e, and x_e are the fluorescence lifetimes, amplitudes, number of decay components, and ground-state mole fraction of the exposed dansyl probes. The corresponding parameters for the buried probes are denoted by a "b" subscript. An analagous expression was used to represent the fractional contribution of the buried probes, $f_b(t)$.

The intrinsic anisotropy decay function for each probe population incorporates separate terms for local rotation of the dansyl probe and overall rotation of the DNA−protein complex. The anisotropy decay for the exposed probes is represented as in eq 4:

$$r_e(t) = \beta_{1e}\exp(-t/\phi_{1e}) + \beta_{2e}\exp(-t/\phi_{2e}) \quad (4)$$

where β_{1e} and ϕ_{1e} are the anisotropy amplitude and correlation time for local rotation, and β_{2e} and ϕ_{2e} are the corresponding quantities for overall tumbling. A similar expression was used to represent the time-dependent anisotropy of the buried dansyl probes. It is assumed that both populations exhibit the same correlation time for overall tumbling ($\phi_{2e} = \phi_{2b}$). Likewise, it is assumed that the correlation time for local rotation is the same for the exposed and buried probes ($\phi_{1e} = \phi_{1b}$), although the amplitude of motion is expected to be much smaller for the buried probes. Accordingly, the anisotropy amplitudes β_{1e}, β_{2e}, β_{1b}, and β_{2b} are floated in the analysis, as described below.

The fractions of exposed and buried dansyl probes, corresponding to the fractions of primer termini bound at the polymerase or 3′-5′ exonuclease sites, respectively, were obtained by fitting the data using one of two methods. In the first method, each anisotropy decay was fitted individually using a Levenberg−Marquardt algorithm, and the fluorescence lifetimes, rotation times, and their associated amplitudes were fixed at the values recovered from a global analysis of Klenow fragment−17/27-mer complexes reported in previous work (*18*). Only the fraction of buried probes (x_b) was allowed to float in each case (note that $x_e = 1 - x_b$), thereby constraining the parameters for the fluorescence anisotropy decays to the previously reported model. In the second method, a global analysis was performed upon multiple data sets obtained for a common primer strand sequence, and the linked rotational decay parameters (β_{1e}, ϕ_{1e}, β_{2e}, ϕ_{2e}, β_{1b}, ϕ_{1b}, β_{2b}, ϕ_{2b}) were optimized across all data sets, while at the same time the fraction of buried probes (x_b) was optimized for each data set. For this model, the fluorescence lifetime parameters were fixed at the previously determined values (*18*). For both models, the anisotropy data were assigned appropriate weighting factors according to the values of $I_{\parallel}(t)$ and $I_{\perp}(t)$ at each time point (*22*). The quality of the fits was judged by the reduced χ^2 values for each data set.

Given that the buried and exposed danysl probes correspond to DNA bound at the 3′-5′ exonuclease site or the polymerase site, respectively, the equilibrium constant describing the partitioning of DNA between the two sites K_{pe}, was computed from the fitted fractions of buried probes as

$$K_{pe} = \frac{x_b}{1 - x_b} \quad (5)$$

RESULTS

Three different primer sequences, differing only in the last six bases at the 3′ terminus, were used to examine the effects of (A+T)-rich sequences on the partitioning of DNA primer/templates between the polymerase and 3′-5′ exonuclease sites of Klenow fragment. Data for the AAAATG primer (the sequence refers to the six terminal bases, written 5′ to 3′) were reported previously (*38*). Here, we report measurements for a sequence containing two AT steps (CGATAT) and a sequence containing a short run of A and T residues with a single AT step (CAATTT). These primers were annealed with either fully or partially complementary template oligonucleotides to form a series of matched and singly mismatched duplex DNA substrates (Table 1). A matched duplex substrate with the primer sequence CAGTTT was also examined. Measurements made upon the matched duplexes indicated that the fluorescence lifetime and anisotropy decays of the dansyl probe are similar for all three primer sequences, with an average fluorescence lifetime of 4 ns and a rotational correlation time of approximately 10 ns (data not shown).

The fluorescence anisotropy decay profiles for the DNA substrates bound to Klenow fragment were fitted to a model incorporating two local environments for the dansyl probe, exposed or buried, corresponding to primer/templates occupying the polymerase site or the 3′-5′ exonuclease site of the enzyme. The parameters for the fluorescence lifetime and rotational decays were fixed at the values used in previous work (*18*) (Table 2). Matched substrate **3** (CGATAT primer) bound to Klenow fragment yielded a fluorescence anisotropy decay that could readily be fitted to the model used previously, allowing only the fraction of buried probes

Table 2: Parameters from Individual and Global Analyses of the Fluorescence Decay Data

	lifetime parameters									
	τ_{1e} (ns)	τ_{2e} (ns)	τ_{3e} (ns)	α_{1e}	α_{2e}	α_{3e}	τ_{1b} (ns)	τ_{2b} (ns)	α_{1b}	α_{2b}
all fits[a]	1.01	4.13	11.9	0.300	0.674	0.026	3.06	18.4	0.700	0.300
	anisotropy parameters									
	ϕ_{1e} (ns)	ϕ_{2e} (ns)	β_{1e}	β_{2e}	ϕ_{1b} (ns)	ϕ_{2b} (ns)	β_{1b}	β_{2b}		
individual fits[a]	1.24	57.2	0.110	0.081	1.24	57.2	0.028	0.208		
global analysis[b]	1.24	65.0	0.130	0.065	1.24	65.0	0.028	0.240		

[a] Taken from the results of Carver et al. (*18*). [b] Obtained from a global fit of the anisotropy decays for substrates **5** and **6** (Table 2). See text for details.

Table 3: Two-State Analysis for Dansyl Probes Attached to DNA[a]

substrate	terminal sequence[b]	x_b[c]	χ_r^2[d]	K_{pe}[e]
1	-AAAATG-3′ -TTTTACA-	0.06	1.15	0.06[f]
2	-AAAATG-3′ -TTTTA$_G$A-	0.22	1.05	0.28[f]
3	-CGATAT-3′ -GCTATAA-	0.11	1.30	0.12
4	-CGATAT-3′ -GCTAT$_T$A-	0.19	1.26	0.23
5	-CAATTT-3′ -GTTAAAA-	0.57 (0.43)[g]	1.72 (1.03)[g]	1.33 (0.75)[g]
6	-CAATTT-3′ -GTTAA$_T$A-	0.26 (0.23)[g]	2.41 (1.30)[g]	0.35 (0.30)[g]
7	-CAGTTT-3′ -GTCAAAA-	0.03	1.18	0.03

[a] Fluorescence anisotropy decays were fitted to eq 2 using a common set of fluorescence lifetime and rotational decay parameters unless otherwise indicated. [b] The bases near the primer 3′ terminus (top strand) of substrates **1**−**7** are shown. See Table 1 for complete DNA sequences. [c] Fitted fraction of buried dansyl probes. [d] Reduced χ^2 value for best fit. [e] Equilibrium constant for partitioning of DNA between the polymerase and 3′-5′ exonuclease sites (eq 5). [f] Lam et al. (*38*). [g] Results of anisotropy fits using an optimized set of rotational parameters for substrates **5** and **6**. See text for details.

to float (Table 3). The resulting value for the fraction of buried probes was used to calculate K_{pe}, the equilibrium constant for partitioning of DNA between the polymerase and 3′-5′ exonuclease sites (Table 3). The corresponding value for the matched AAAATG duplex (substrate **1**), obtained using the same two-state model and parameters, is included in Table 3 for comparison. It can be seen that substrates **1** and **3** both partition in favor of the polymerase site and yield similar values of K_{pe} (0.06 and 0.12, respectively). The difference in the K_{pe} values for substrates **1** and **3** (Table 3) may reflect the different melting capacities of these sequences, since binding of DNA at the 3′-5′ exonuclease site appears to require unwinding/melting of the primer 3′ terminus (*9*, *11*, *12*, *23*). When the CGATAT primer is paired with a mismatched template to form a single 3′ terminal mismatch (substrate **4**), the K_{pe} value increases by 2-fold (Table 3). A similar effect was previously observed for the mismatched AAAATG duplex bound to Klenow fragment (the K_{pe} value is included in Table 3 for comparison, substrate **2**).

The CAATTT primer sequence, however, displays unusual characteristics. The anisotropy decay profile observed for

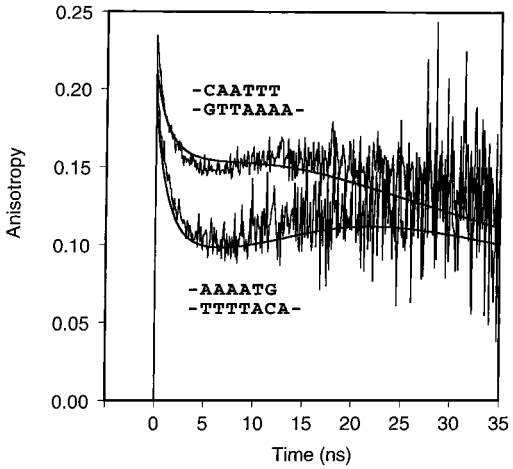

FIGURE 1: Fluorescence anisotropy decay profiles of dansyl-labeled 17/27-mer oligonucleotides bound to D424A Klenow fragment. The decays are labeled according to the DNA sequence near the primer 3′ terminus. See Table 1 for complete DNA sequences. The fitted curves (solid lines) are for individual fits to a two-state model, with the lifetime and rotational decay parameters fixed at the values determined in a previous study (*18*; Table 2). The anisotropy decay profile for the matched terminal sequence AAAATG/TTTTAC fits well to the previously reported model ($\chi_r^2 = 1.15$), whereas the data for the CAATTT/GTTAAA sequence fit poorly ($\chi_r^2 = 1.7$). The displacement between the two curves indicates that a significantly higher fraction of dansyl probes exist in the buried state for the CAATTT/GTTAAA terminal sequence.

the matched duplex (substrate **5**) bound to Klenow fragment is shifted upward relative to the other matched seqences, consistent with a larger fraction of buried dansyl probes (Figure 1). Furthermore, the data are fitted poorly using the fluorescence lifetime and rotational parameters established in previous work (Figure 1). The anisotropy decay for the related substrate containing a single 3′ terminal mismatch (substrate **6**) is also poorly fitted to the original two-state model ($\chi_r^2 = 2.4$). To obtain better fits for substrates **5** and **6**, both data sets were fitted globally, allowing the rotational parameters to adopt new values. The fluorescence lifetime parameters were not changed, however. Excellent fits were obtained for both the matched and mismatched substrates (Figure 2). The resulting rotational parameters (Table 2) are slightly different from those that were previously assigned to the exposed and buried populations of dansyl probes. These results suggest that the local environments for each probe population are somewhat different than for other DNA sequences, indicative of a different footprint of Klenow fragment upon the primer/templates containing the CAATTT sequence. Alternatively, binding of the protein could indirectly affect the dansyl fluorescence by inducing structural changes in the DNA duplex in the vicinity of the dansyl probe. To rule out possible undetected artifacts that might have occurred in DNA synthesis, substrate **5** was resynthesized and purified, giving the same fluorescence anisotropy decay as observed for Klenow fragment complexed with the original primer/template.

The K_{pe} value for the matched CAATTT duplex (**5**) bound to Klenow fragment is much larger than observed for the other (A+T)-rich primers, irrespective of how the anisotropy decay is analyzed (Table 3), showing that this sequence increases partitioning of DNA into the 3′-5′ exonuclease site. More significantly, the related mismatched substrate (**6**), containing a single 3′ terminal mismatch, gives a *smaller*

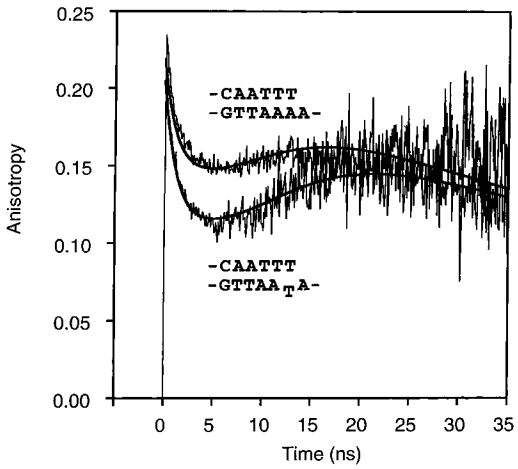

FIGURE 2: Fluorescence anisotropy decay profiles for complexes of D424A Klenow fragment with 17/27-mer primer/templates containing the CAATTT primer. The decays are labeled according to the base sequence near the primer 3′ terminus. See Table 1 for complete sequences of the 17/27-mers. The fitted curves (solid lines) are from a global fit to a two-state model, with the rotational parameters for each probe population linked across both data sets (see Table 2 for fitted parameters). The fitted fractions of buried dansyl probes, corresponding to the fractions of 3′ termini bound at the 3′-5′ exonuclease site, are $x_b = 0.43$ (matched sequence) and $x_b = 0.23$ (single mismatch).

fraction of buried dansyl probes than the matched sequence (Table 3). The resulting value of K_{pe}, however, is comparable to the results observed for single mismatches in the context of the other (A+T)-rich primer sequences (Table 3). These results suggest that the matched duplex sequence CAATTT/GTTAAA adopts an unusual conformation that causes the DNA to partition in favor of the 3′-5′ exonuclease site, and that this conformation is not present when the sequence is altered by a single mismatch.

To confirm that the high occupancy of the 3′-5′ exonuclease site is specific to the CAATTT/GTTAAA duplex sequence, a new primer/template was synthesized in which the central AT step was replaced by a GT step (terminal sequence CAGTTT/GTCAAA, substrate **7**). The anisotropy decay for this substrate fits well to the original model and yields a K_{pe} value of 0.03 (Table 3), showing that the DNA is bound predominantly at the polymerase site.

DISCUSSION

We have identified a perfectly base-paired DNA sequence that promotes binding of a DNA primer/template to the proofreading 3′-5′ exonuclease site of Klenow fragment. In a previous study, we examined the effects of mismatches upon partitioning of DNA substrates between the polymerase and 3′-5′ exonuclease sites (*18*). Time-resolved anisotropy decays for dansyl-labeled 17/27-mers exhibited an unusual "dip and rise" pattern that could be fitted to an expression incorporating two local environments for the dansyl probes: a solvent-exposed environment where the probes had greater freedom of motion and shorter emission lifetimes, and a buried environment where the probes were motionally restricted and had longer emission lifetimes (*18*). The population of buried probes increased as mismatches were introduced into the primer/templates, demonstrating that the buried probes correspond to DNA bound at the 3′-5′ exonuclease site. An earlier study in which a dansyl-labeled DNA substrate was immobilized at the polymerase site by an epoxy-modified residue at the primer 3′ terminus established that the exposed dansyl probes correspond to DNA bound to the polymerase site of the enzyme (*21*).

The general conclusion of our previous study was that mismatches promoted binding of the primer 3′ terminus to the 3′-5′ exonuclease site, consistent with a primer terminus that is more easily melted (*18*). In the present work, we have extended the analysis to include several other sequences, and to determine if sequence variation alone can induce changes in the nature and relative distribution of binding modes of DNA substrates bound to Klenow fragment. The anisotropy decays of three different base-paired 17/27-mer duplexes containing an upstream dansyl probe were compared: primer sequences terminating in AAAATG, CGATAT, and CAATTT. The time-resolved fluorescence anisotropy decays of the first two sequences could be analyzed in terms of the two-state model established in previous work, whereas the decay of the last sequence, CAATTT, exhibited a different profile, consistent with a larger fraction of buried dansyl probes. Furthermore, these data did not fit well to the fluorescence lifetime and rotational decay parameters used for the other DNA sequences. The anisotropy decays for this substrate and a related primer/template containing a single 3′ terminal mismatch were globally analyzed, yielding a new set of self-consistent rotational decay parameters that provided a good fit for the CAATTT primer sequence. It was found that regardless of how the data were fit, the CAATTT sequence had a very unusual effect upon the distribution of the two states of the dansyl probes: more of the probes were in the buried, hyperfluorescent environment for the matched substrate compared with the mismatched substrate (Table 3). This result runs counter to the observations made for other primer/templates containing single base pair mismatches, for which the occupancy of the 3′-5′ exonuclease site is always larger than for the corresponding matched sequence (Table 3; see also *18*). The simplest interpretation of this result is that the matched sequence CAATTT/GTTAAA contains some feature that favors binding to the 3′-5′ exonuclease site within the polymerase relative to other sequences with the same (A+T) content (Table 3).

Short runs of A and T residues have been shown to affect both the flexibililty and local geometry of the DNA double helix. In particular, sequence motifs of the form 5′-A_nT_m-3′, where $n + m \geq 4$, are known to be intrinsically curved (reviewed in *15* and *24*). Although the structural basis of sequence-directed curvature of DNA is still under investigation, crystallographic and NMR studies have shown that the local helix geometry of these A-tract regions differs significantly from canonical B-DNA (*25*). An A-tract (5′-AATTT-3′) is present in the matched sequence CAATTT/GTTAAA, but absent from the alternating sequence CGATAT/GCTATA. Therefore, a logical explanation for the large differences observed in the partitioning of these two sequences between the polymerase and 3′-5′ exonuclease sites is that the A-tract sequence causes an altered helical structure to exist near the primer 3′ terminus. This hypothesis is supported by the results for the closely related matched terminal sequence CAGTTT/GTCAAA (**7**), in which a single base pair substitution within the A-tract causes the DNA terminus to partition in favor of the polymerase site rather

than the 3′-5′ exonuclease site (Table 3). Moreover, our results show that the effect of an A-tract sequence on the partitioning of DNA between polymerase and 3′-5′ exonuclease sites is specific to the size and location of the tract within the primer/template. For example, the mismatched sequence CAATTT/GTTAAT (**6**) contains a small A-tract (5′-AATT-3′), displaced one base upstream from the primer 3′ terminus, yet the K_{pe} value for this sequence is consistent with those measured for other singly mismatched DNA sequences (Table 3). Similarly, the matched sequence AAAATG/TTTTAC (**1**) contains an A-tract (5′-AAAAT-3′), also displaced from the primer terminus, yet the K_{pe} value lies in the normal range for a matched sequence. Thus, our results suggest that the A-tract must contain at least 5 bp and encompass the 3′ terminus in order to cause the DNA substrate to partition in favor of the 3′-5′ exonuclease site.

In principle, there are two possible mechanisms by which an A-tract sequence element at the primer 3′ terminus could favor binding of a DNA substrate at the 3′-5′ exonuclease site over binding at the polymerase site. First, the A-tract may enhance the binding of the primer/template to the 3′-5′ exonuclease site, without changing the intrinsic affinity for the polymerase site. Such increased binding to the 3′-5′ exonuclease site would imply a less stable duplex terminus, since binding of duplex DNA to the 3′-5′ exonuclease site requires localized melting and unwinding of DNA (*9*−*12*). However, spectroscopic and calorimetric melting studies of A-tract DNA indicate that the stability of these regions is similar to that of non A-tract DNA with similar (A+T) content (*26*, *27*). Moreover, if the high occupancy of the 3′-5′ exonuclease site is due to an increased melting capacity of the AATTT/TTAAA element, then it would be expected that the corresponding mismatched sequence AATTT/TTAAT would exhibit an even greater preference for the 3′-5′ exonuclease site because it is presumably less stable. In fact, the reverse is true (Table 3). Second, the A-tract might adopt an unusual structure that is disruptive to binding of the primer/template to the polymerase site, without changing the affinity for the 3′-5′ exonuclease site. In fact, A-tract regions in duplex DNA are characterized by unusual helix structural parameters, including high propellor twist, negative base pair inclination with respect to the helix axis, and a narrowing of the minor groove (*28*−*30*). For example, the duplex $[d(CCAAATTTGG)]_2$ has been shown to adopt a rigid, modified B-form structure, termed B′, in which the minor groove is considerably narrowed, facilitating its recognition by minor groove binding drugs such as distamycin and leading to different patterns of thymine dimer formation and metal binding (*31*, *32*). EPR spectroscopic studies of spin-labeled duplex oligomers have shown that the sequence AAATT, but not AATT, induces a structural distortion in duplex DNA, attributed to a bend toward the major groove (*33*). Thus, increased helix rigidity, sequence-directed bending, constriction of the minor groove, or a different spacing of the backbone phosphates could potentially lead to unfavorable interactions between the sequence AATTT/TTAAA and the polymerase active site of Klenow fragment. Therefore, although our results do not directly distinguish the two mechanisms outlined above, the most reasonable inference to be drawn from the available data is that the AATTT element affects partitioning by disrupting the binding of the DNA substrate at the polymerase site.

A recent crystal structure of duplex DNA bound to the polymerase domain of Taq DNA polymerase provides some clues as to how sequence-dependent structural effects could inhibit the binding of DNA to the polymerase domain of Klenow fragment (*34*). The structures of the polymerase domains of Klenow fragment and Taq polymerase are almost identical, suggesting that the mode of DNA binding should be the same in each case (*17*, *35*). A prominent feature of the Taq polymerase−DNA complex is the unusual structure of the bound DNA duplex, which is intermediate between the A and B forms. In particular, the minor groove is much wider than for B-DNA, which allows access for protein side chains to hydrogen-bond to the O2 of pyrimidines and the N3 of purines at the 3′ terminus. The tendency of an A-tract to constrict the minor groove may prevent the proper formation of these DNA−protein contacts and thereby weaken the binding of a DNA substrate to the polymerase active site. This would explain why an A-tract sequence displaced just one base pair upstream from the primer 3′ terminus appears to be less disruptive to binding at the polymerase site, as noted above. Alternatively, an altered spacing between phosphate groups could disrupt the network of hydrogen bonds between the protein and the DNA backbone (*34*).

Sensitivity toward sequence-dependent variations in helix geometry may be a common feature of enzymes that use duplex DNA as a substrate but do not recognize base sequence per se. Drew and others (*14*, *36*) have observed that the enzyme DNAse I cleaves duplex DNA poorly at homopolymeric dA·dT runs containing a central AT step. These effects were explained by assuming that the enzyme prefers a DNA substrate with a minor groove of average width. Shatzky-Schwartz et al. (*13*) have shown that the activities of several DNA-processing enzymes, including DNase I and the exonucleases BAL31 and exoIII, are markedly impaired by the presence of repeated A-tract sequences (5′-A_4T_4-3′) within their duplex DNA substrates. These effects were attributed to a reduced binding affinity of the enzymes for bent regions of DNA. Our results suggest that for an enzyme with two DNA-binding sites, such as Klenow fragment, the presence of an A-tract structure can selectively inhibit DNA binding at one of the sites. Weak binding of the polymerase site to a duplex terminus within an A-tract region could potentially reduce the rate of nucleotide incoporation during replicative DNA synthesis, suggesting that the polymerase may stall during the copying of such sequence elements. In fact, Lavigne et al. (*37*) have recently shown that the reverse transcriptase from HIV-1 terminates plus strand synthesis at an A_nT_m ($n + m = 7$) sequence element. While sequence effects on nucleotide incorporation have been discussed mainly in terms of differences in base stacking energies (*4*, *5*, *7*), the present results suggest that sequence-directed alterations in DNA helix geometry could also modulate the enzymatic activities of a DNA polymerase.

CONCLUSIONS

We have investigated the importance of DNA sequence and structure in determining the partitioning of DNA substrates between the polymerase and 3′-5′ exonuclease sites of Klenow fragment. We found that a particular base-paired

sequence tends to partition into the 3′-5′ exonuclease site to a greater extent than an analogous mispaired sequence, suggesting that the melting capacity of the primer terminus is only one of several factors influencing partitioning: narrowing of the minor groove, altered spacing between phosphate groups, or other local distortions in DNA helix geometry may change the distribution of binding modes for a primer 3′ terminus within the polymerase. These results suggest that it should be possible to define the structure/function relationships that are involved in polymerase−DNA interactions that contribute to DNA replication fidelity.

ACKNOWLEDGMENT

We thank Wai-Chung Lam for assistance with some of the time-resolved fluorescence anisotropy measurements.

REFERENCES

1. Kunkel, T. A. (1988) *Cell 53*, 837−840.
2. Echols, H., and Goodman, M. F. (1991) *Annu. Rev. Biochem. 60*, 477−511.
3. Goodman, M. F., Creighton, S., Bloom, L. B., and Petruska, J. (1993) *Crit. Rev. Biochem. Mol. Biol. 28*, 83−126.
4. Petruska, J., and Goodman, M. F. (1985) *J. Biol. Chem. 260*, 7533−7539.
5. Mendelman, L. V., Boosalis, M. S., Petruska, J., and Goodman, M. F. (1989) *J. Biol. Chem. 264*, 14415−14423.
6. Joyce, C. M., Sun, X. C., and Grindley, N. D. F. (1992) *J. Biol. Chem. 267*, 24485−24500.
7. Bloom, L. B., Otto, M. R., Beechem, J. M., and Goodman, M. F. (1993) *Biochemistry 32*, 11247−11258.
8. Bloom, L. B., Otto, M. R., Eritja, R., Reha-Krantz, L. J., Goodman, M. F., and Beechem, J. M. (1994) *Biochemistry 33*, 7576−7586.
9. Brutlag, D., and Kornberg, A. (1972) *J. Biol. Chem. 247*, 241−248.
10. Freemont, P. S., Friedman, J. M., Beese, L. S., Sanderson, M. R., and Steitz, T. A. (1988) *Proc. Natl. Acad. Sci. U.S.A. 85*, 8924−8928.
11. Beese, L., Derbyshire, V., and Steitz, T. A. (1993) *Science 260*, 352−355.
12. Cowart, M., Gibson, K. J., Allen, D. J., and Benkovic, S. J. (1989) *Biochemistry 28*, 1975−1983.
13. Shatzky-Schwartz, M., Hiller, Y., Reich, Z., Ghirlando, R., Weinberger, S., and Minsky, A. (1992) *Biochemistry 31*, 2339−2346.
14. Drew, H. R., and McCall, M. J. (1990) in *DNA Topology and its Effects*, pp 1−56, Cold Spring Harbor Laboratory Press, Cold Spring Harbor, NY.
15. Hagerman, P. J. (1990) *Annu. Rev. Biochem. 59*, 755−781.
16. Joyce, C. M., and Steitz, T. A. (1994) *Annu. Rev. Biochem. 63*, 777−822.
17. Ollis, D. L., Brick, P., Hamlin, R., Xuong, N. G., and Steitz, T. A. (1985) *Nature 313*, 762−766.
18. Carver, T. E., Hochstrasser, R. A., and Millar, D. P. (1994) *Proc. Natl. Acad. Sci. U.S.A. 91*, 10670−10674.
19. Derbyshire, V., Grindley, N. D. F., and Joyce, C. M. (1991) *EMBO J. 10*, 17−24.
20. Allen, D. J., Darke, P. L., and Benkovic, S. J. (1989) *Biochemistry 29*, 3612−3621.
21. Guest, C. R., Hochstrasser, R. A., Dupuy, C. G., Allen, D. J., Benkovic, S. J., and Millar, D. P. (1991) *Biochemistry 30*, 8759−8770.
22. O'Connor, D. V., and Philips, D. R. (1988) *Time-Correlated Single Photon Counting*, p 271, Academic Press, London.
23. Derbyshire, V., Freemont, P. S., Sanderson, M. R., Beese, L., Friedman, J. M., Joyce, C. M., and Steitz, T. A. (1988) *Science 240*, 199−201.
24. Crothers, D. M., Haran, T. E., and Nadeau, J. G. (1990) *J. Biol. Chem. 265*, 7093−7096.
25. Young, M. A., Ravishanker, G., Beveridge, D. L., and Berman, H. M. (1995) *Biophys. J. 68*, 2454−2468.
26. Chan, S. S., Breslauer, K. J., Hogan, M. E., Kessler, D. J., Austin, R. H., Ojemann, J., Passner, J. M., and Wiles, N. C. (1990) *Biochemistry 29*, 6161−6171.
27. Park, Y.−W., and Breslauer, K. J. (1991) *Proc. Natl. Acad. Sci. U.S.A. 88*, 1551−1555.
28. Nelson, H. C. M., Finch, J. T., Luisi, B. F., and Klug, A. (1987) *Nature 330*, 221−226.
29. Yoon, C., Prive, G. G., Goodsell, D. S., and Dickerson, R. E. (1988) *Proc. Natl. Acad. Sci. U.S.A. 85*, 6332−6336.
30. Burkhoff, A. M., and Tullius, T. D. (1987) *Cell 48*, 935−943.
31. Gueron, M., Charretier, E., Hagerhorst, J., Kochoyan, M., Leroy, J. L., and Moraillon, A. (1990) in *Structure and Methods.* (Sarma, R. H., and Sarma, M. H., Eds.) *Vol. 3: DNA and RNA*, pp 207−224, Adenine Press, New York.
32. Demidov, V. V., and Potaman, V. N. (1993) *Nucleic Acids Res. 21*, 2691−2696.
33. Bobst, E. V., Keyes, R. S., Cao, Y. Y., and Bobst, A. M. (1996) *Biochemistry 35*, 9309−9313.
34. Eom, S. H., Wang, J., and Steitz, T. A. (1996) *Nature 382*, 278−281.
35. Kim, Y., Eom, S. H., Wang, J., Lee, D.-S., Suh, S. W., and Steitz, T. A. (1995) *Nature 376*, 612−616.
36. Drew, H. R., and Travers, A. A. (1984) *Cell 37*, 491−502.
37. Lavigne, M., Roux, P., Buc, H., and Schaeffer, F. (1997) *J. Mol. Biol. 266*, 507−524.
38. Lam, W.-C., Van der Schans, E. J. C., Joyce, C. M., and Millar, D. P. (1998) *Biochemistry* (in press).

BI9720843